

Kolmogorov's refined similarity hypothesis: consequences from an exact two-point equation for isotropic turbulence

H. Yao

Department of Mechanical Engineering & Institute for Data Intensive Engineering & Science, Johns Hopkins University

P. K. Yeung

Department of Aerospace Engineering and Mechanical Engineering, Georgia Institute of Technology

T. A. Zaki and C. Meneveau*

Mechanical Engineering & IDIES, Johns Hopkins University

(Dated: July 14, 2023)

In order to describe intermittency and anomalous scaling in turbulence, Kolmogorov's second refined similarity hypothesis (KRSH) connects statistics of velocity increments to those of the rate of dissipation ϵ_r , averaged in a sphere at a scale r in the inertial range. We explore this classic hypothesis in light of the generalized Kolmogorov-Hill equation (GKHE) derived exactly from the Navier-Stokes equations, and in which ϵ_r appears explicitly. When evaluated using conditional averaging based on ϵ_r , analysis of Direct Numerical Simulations data at various Reynolds numbers shows that the energy cascade rate indeed equals ϵ_r . Conditional higher-order moments also support KRSH, while an "inverse KRSH" is not supported by data. Finally, results confirm KRSH even when applied separately to positive (forward) and negative (inverse) cascade regions of the flow.

The classic description of the energy cascade in turbulent flows states that the turbulent kinetic energy is extracted from large-scale eddies, transferred to smaller scale eddies (the forward cascade), and finally dissipated into heat due to viscous friction [1]. What is known from the Navier-Stokes equations is that a global averaging of the Kolmogorov equation for two-point longitudinal velocity increments connects third-order moments to the overall mean rate of viscous dissipation via the celebrated $-4/5$ law [2, 3],

$$\langle \delta u_L^3 \rangle \equiv \langle ([\mathbf{u}(\mathbf{x} + \mathbf{r}) - \mathbf{u}(\mathbf{x})] \cdot \mathbf{r}/r)^3 \rangle = -\frac{4}{5} r \langle \epsilon \rangle. \quad (1)$$

Here $\langle \dots \rangle$ denotes statistical averaging, δu_L is the longitudinal velocity increment, ϵ is the viscous dissipation rate, and $r = |\mathbf{r}|$ is assumed to be well inside the inertial range of turbulence. Eq. (1) means that in the inertial range, $-(5/4)\langle \delta u_L^3 \rangle/r$ can be interpreted as the energy transfer rate, that it is constant with r , and that the average transfer direction is from large to small scales. However, it is well known that this relation does not hold locally, as δu_L and the dissipation rate display strong variability and intermittency [3–5]. In order to describe intermittency and anomalous scaling, Kolmogorov's second refined similarity hypothesis (KRSH) [4] connects the statistical distributions of velocity increments to those of the local rate of dissipation ϵ_r , defined as the point-wise dissipation averaged in a ball of diameter r . Specifically, the KRSH states that velocity increments and ϵ_r are connected via a universal random variable V according to $\delta u_L = V(r\epsilon_r)^{1/3}$. The second hypothesis, for r in the

inertial range, states that the statistics of V are independent of r and ϵ_r . A direct consequence is that moments of δu_L , conditionally averaged on ϵ_r are proportional to corresponding powers of $(r\epsilon_r)^{1/3}$ when r is in the inertial range of high Reynolds number turbulence. The validity of KRSH has received strong support from early experimental measurements in which the dissipation ϵ_r had to be approximated by lower-dimensional data (e.g., [6, 7]) and also from later analyses based on 3D data, in which ϵ_r could be evaluated fully, from simulations [8, 9] as well as more recently based on 3D experimental data [10].

Most prior studies have started out with the KRSH formulated as a hypothesis inspired by dimensional analysis and sound physical reasoning. However, direct connections between KRSH and first-principles Navier-Stokes equations have been lacking. In 2002, Hill [11, 12] derived an equation which here will be denoted as the generalized Kolmogorov-Hill equation (GKHE). Before averaging, the GKHE is fully local, accounting for the evolution of velocity increment magnitude (square) at a specific physical location and length scale, and it also incorporates effects of viscous dissipation, viscous transport, convection, and pressure [11, 12]. The GKHE is derived from the incompressible Navier-Stokes equations written at two points [11, 12]. Other variants of the GKHE which take into account the effects of mean flow, mean shear, mean-flow advection and anisotropy have since been developed [13–18]. The instantaneous GKHE with no mean flow and neglecting the forcing term takes the form

$$\begin{aligned} \frac{\partial \delta u_i^2}{\partial t} + u_j^* \frac{\partial \delta u_i^2}{\partial x_j} &= -\frac{\partial \delta u_j \delta u_i^2}{\partial r_j} - \frac{8}{\rho} \frac{\partial p^* \delta u_i}{\partial r_i} \\ &+ \nu \frac{1}{2} \frac{\partial^2 \delta u_i \delta u_i}{\partial x_j \partial x_j} + 2\nu \frac{\partial^2 \delta u_i \delta u_i}{\partial r_j \partial r_j} - 4\epsilon^* \end{aligned} \quad (2)$$

where $\delta u_i = \delta u_i(\mathbf{X}; \mathbf{r}) = u_i^+ - u_i^-$ is the velocity incre-

* meneveau@jhu.edu

ment vector in the i^{th} Cartesian direction. The superscripts $+$ and $-$ represent two points $\mathbf{x} + \mathbf{r}/2$ and $\mathbf{x} - \mathbf{r}/2$ in the physical domain that have a separation vector $r_i = x_i^+ - x_i^-$ and middle point $x_i = (x_i^+ + x_i^-)/2$. The superscript $*$ denotes the average value between two points, e.g., the average dissipation is defined as $\epsilon^* = (\epsilon^+ + \epsilon^-)/2$, and what in this paper we denote as ϵ is the ‘‘pseudo-dissipation’’ defined at every point as $\epsilon = \nu(\partial u_i/\partial x_j)^2$.

As already noted by Hill [§3.5 in 12], in order to make connection to the RKSH and ϵ_r , Eq. 2 at any point \mathbf{x} can be integrated over a sphere in the scale \mathbf{r} -space, up to a radius $r/2$ (diameter equal to r). The resulting equation is divided by the volume of the sphere ($V_r = \frac{4}{3}\pi(r/2)^3$) and a factor of 4, which yields its integrated form,

$$\frac{\tilde{d}k_r}{dt} = \Phi_r + P_r + D_r - \epsilon_r, \quad \text{where} \quad (3)$$

$$\epsilon_r(\mathbf{x}) \equiv \frac{1}{V_r} \iiint_{V_r} \epsilon^*(\mathbf{x}, \mathbf{r}) d^3 \mathbf{r}_s \quad (4)$$

is the r -averaged rate of dissipation envisioned in the RKSH with the radius vector $\mathbf{r}_s = \mathbf{r}/2$ being integrated up to magnitude $r/2$, and

$$\Phi_r \equiv -\frac{3}{4r} \frac{1}{S_r} \oint \delta u_i^2 \delta u_j \hat{r}_j dS = -\frac{3}{4r} [\delta u_i^2 \delta u_j \hat{r}_j]_{S_r} \quad (5)$$

is interpreted as the local energy cascade rate in the inertial range at position \mathbf{x} . Note that Gauss theorem is used to integrate the first term on the RHS of Eq. 2 over the r -sphere’s surface, with area element $\hat{r}_j dS$, with $\hat{\mathbf{r}} = \mathbf{r}/|\mathbf{r}|$, and $S_r = 4\pi(r/2)^2$ the sphere’s overall area (care must be taken as the Gauss theorem applies to the sphere’s radius vector $\mathbf{r}_s = \mathbf{r}/2$ and $\partial_r = 2\partial_{r_s}$). Averaging over the surface S_r is denoted by $[\dots]_{S_r}$.

Other terms in Eq. 3 include

$$\frac{\tilde{d}k_r}{dt} \equiv \frac{1}{2V_r} \iiint_{V_r} \left(\frac{\partial \delta u_i^2/2}{\partial t} + u_j^* \frac{\partial \delta u_i^2/2}{\partial x_j} \right) d^3 \mathbf{r}_s, \quad (6)$$

which is the local average of advective rate of change of kinetic energy $k_r = (1/2V_r) \int_{V_r} \frac{1}{2} \delta u_i^2 d^3 \mathbf{r}_s$ at all scales smaller or equal to r (the factor 2 in the denominator in front of the volume integration accounts for the double-counting of point pairs), and

$$P_r \equiv -\frac{6}{r} \frac{1}{S_r} \oint \frac{1}{\rho} p^* \delta u_j \hat{r}_j dS \quad (7)$$

is a surface averaged pressure work term at scale r . The term $D_r = \nu/(8V_r) \int_{V_r} [\partial^2 \delta u_i^2/\partial x_j^2 + 4\partial^2 \delta u_i^2/\partial r_j^2] d^3 \mathbf{r}_s$ represents viscous diffusion of kinetic energy both in position and scale space. We consider r to be in the inertial range and will therefore neglect D_r . Equation 3 is local (valid at any point \mathbf{x} and time t), and each of the terms

in the equation can be evaluated from data according to their definition using a sphere centered at any middle point x_i . Without the viscous, pressure and unsteady terms, Eq. 3 is similar to the ‘‘local 4/3-law’’ obtained by Duchon & Robert [19] and discussed by Eyink [20, 21], relating Φ_r and ϵ_r in the context of energy dissipation in the limit of zero viscosity.

A reformulation of the KRSH in the present context is that the statistics of Φ_r (i.e., of $(-3/4r)[\delta u_i^2 \delta u_j \hat{r}_j]_{S_r}$) only depend on the statistics of ϵ_r (i.e. that $\Phi_r = V_\Phi \epsilon_r$ with V_Φ being a random variable with universal statistics independent of r and ϵ_r) in the inertial range. In particular, the conditional average of the cascade rate obeys $\langle \Phi_r | \epsilon_r \rangle = \epsilon_r$. But referring back to the local GKHE (Eq. 3), we may now take its conditional average and write

$$\langle \tilde{d}k_r/dt | \epsilon_r \rangle = \langle \Phi_r | \epsilon_r \rangle + \langle P_r | \epsilon_r \rangle - \epsilon_r, \quad (8)$$

considering that of course $\langle \epsilon_r | \epsilon_r \rangle = \epsilon_r$ and neglecting the viscous diffusion term. Hence, a consequence of the KRSH together with the GKHE equation is that the conditional average of $W_r \equiv \tilde{d}k_r/dt - P_r$ must vanish, i.e. $\langle W_r | \epsilon_r \rangle = 0$, either when both terms are combined in W_r , or perhaps they vanish also individually, $\langle \tilde{d}k_r/dt | \epsilon_r \rangle = 0$ and $\langle P_r | \epsilon_r \rangle = 0$.

In this letter, we investigate whether data support the KRSH in the context of the GKHE and whether the conditional moments of Φ_r and of the combined unsteady and pressure terms W_r conform to the predictions of the KRSH. We evaluate terms using data from Direct Numerical Simulation of isotropic turbulence at $R_\lambda \approx 1,250$ that used 8,192³ grid-points in a $(2\pi)^3$ periodic domain (data obtained from the JHTDB database [22, 23]). Taking dissipation as an example, panel (a) in figure 1 shows point-wise normalized dissipation $\epsilon(\mathbf{x})/\langle \epsilon \rangle$ computed on a planar cut across the data (the plane shown corresponds to 500×500 grid points). Panel (b) of figure 1 shows a sphere with diameter r . Velocity and gradient data are obtained using JHTDB’s *Getfunction* tools.

The cascade rate (or energy flux) Φ_r is measured using surface averaging of $\delta u_i^2 \delta u_j \hat{r}_j$ over a sphere of diameter r . When this solid angular averaging yields a negative result, i.e. when the average of the δu_i^2 -weighted radial component of δu_j is negative and thus points inwards, $\Phi_r > 0$ and the energy flux transfers energy towards smaller scales within the integration surface, indicating a local forward cascade. Conversely, when $\Phi_r < 0$, the energy flux transfers outward from the spherical surface, indicating a local inverse cascade. On a global average, $\langle \Phi_r \rangle = \langle \epsilon \rangle > 0$ as dictated by the -4/5 relation.

Figure 2 shows the measured conditional average $\langle \Phi_r | \epsilon_r \rangle$ as function of ϵ_r . Statistics are computed using 2,000,000 randomly distributed spheres across the entire 8192³ isotropic turbulence dataset (isotropic8192) [23]. The analysis considers two length scales in the inertial range and one approaching the viscous range, namely $r = 0.024\ell = 60\eta$, $r = 0.018\ell = 45\eta$, and $r = 0.012\ell = 30\eta$, respectively, where $\ell = 1.24$ is the integral scale and

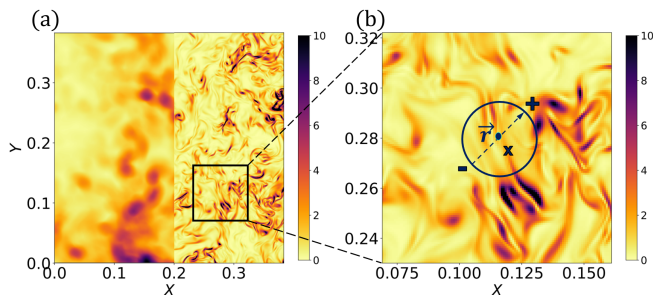


FIG. 1. (a) Spatial distribution of local dissipation rate normalized by $\langle \epsilon \rangle$ on a plane in a small subset of isotropic turbulence at $R_\lambda = 1,250$. The left half portion shows ϵ_r distribution obtained from spherical volume averaging. (b) Zoomed-in portion of panel (a) also showing a sphere with a diameter $r = 45\eta$ marked as the black circle. The black dash arrow represents the separation vector \mathbf{r} . The center of the sphere is the middle point \mathbf{x} between two points + and -.

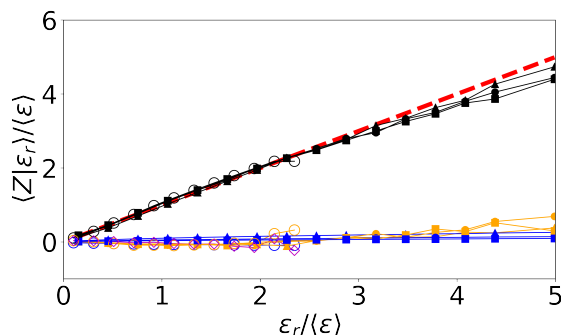


FIG. 2. Conditional averages of terms in the GKH equation (but not including the rate of change term) based on local dissipation ϵ_r , i.e., $Z = \Phi_r$ (black symbols and lines), $Z = P_r$ (yellow symbols and lines), $Z = D_r$ (blue symbols and lines). The red line indicates the value of ϵ_r . Different symbols denote different scales $r/\ell = 0.012$ (triangles), 0.018 (circles, 45η) and 0.024 (squares). Solid symbols: Data from DNS of forced isotropic turbulence at $R_\lambda = 1,250$. Open circles: Data from DNS at $R_\lambda = 430$ at $r/\ell = 0.092$ (45η), for which time dependency can be evaluated and thus including the unsteadiness term $Z = \tilde{d}k_r/dt$ (purple diamond, near zero). All terms are normalized with $\langle \epsilon \rangle$.

the Kolmogorov scale is $\eta = (\nu^3/\langle \epsilon \rangle)^{1/4} = 4.98 \times 10^{-4}$. It is immediately apparent that the dominant terms are $\langle \Phi_r | \epsilon_r \rangle$ (black dots) and ϵ_r itself (red dash line with unit slope). These are equal for most of the range of ϵ_r for which reliable statistics can be collected. The good collapse $\langle \Phi_r | \epsilon_r \rangle \approx \epsilon_r$ provides further support for the KRSK in the context of terms appearing in the GKHE. Also plotted in Fig. 2 are the conditional averages of the pressure term, $\langle P_r | \epsilon_r \rangle$, and the viscous term, $\langle D_r | \epsilon_r \rangle$. We can see that the contribution of the pressure term (yellow squares) is negligible at all three length scales over most of the range. The viscous term (solid blue lines) is also negligibly small. Approaching the largest values of $\epsilon_r/\langle \epsilon \rangle$ we observe saturation of Φ_r that is compensated

by small rise of the pressure term.

It should be noted that the isotropic8192 dataset does not contain snapshots sufficiently close in time to compute time derivatives to evaluate $\langle \tilde{d}k_r/dt | \epsilon_r \rangle$. However, based on Eq. 8, we can conclude that $\langle \tilde{d}k_r/dt | \epsilon_r \rangle \approx 0$, given that $\langle P_r | \epsilon_r \rangle \approx 0$, $\langle V_r | \epsilon_r \rangle \approx 0$, and $\langle \Phi_r | \epsilon_r \rangle \approx \epsilon_r$. To verify this result via explicit measurement, we computed the terms in Eq. 8 using the isotropic1024 [22]. This dataset has a smaller size of 1024^3 grid points and a lower Reynolds number $R_\lambda = 430$, but includes temporally consecutive snapshots allowing us to calculate time derivatives. Fig. 2 (open symbols) shows that $\langle \Phi_r | \epsilon_r \rangle \approx \epsilon_r$ still holds very well at this lower Reynolds number, that the pressure and viscous terms are again close to zero and that $\langle \tilde{d}k_r/dt | \epsilon_r \rangle \approx 0$. We conclude that the data provide strong direct support to the RKSJ relating Φ_r and ϵ_r and that the conditional averages of the pressure and unsteadiness terms vanish in the inertial range, as required from the conditionally averaged GKH equation. As mentioned above, at large values, a saturation of the KRSJ prediction is observed. Such deviations can be expected since δu cannot exceed significantly the outer velocity scale, i.e. the rms velocity $u' \sim (\langle \epsilon \rangle \ell)^{1/3}$. This leads to saturation of KRSJ at values of $\Phi_r \sim u'^3/r \sim \langle \epsilon \rangle (\ell/r)$. Indeed cases at lower ℓ/r show earlier saturation. Only if both r and δu are well inside the inertial range is KRSJ expected to hold.

A further implication of KRSJ relates to higher order moments. It implies that $\langle \Phi_r^q | \epsilon_r \rangle = \langle V_\Phi^q \rangle \epsilon_r^q$ (and $\langle V_\Phi \rangle = 1$ for the case $q = 1$ discussed before). In the inertial range, since $\Phi_r = \epsilon_r + W_r$ locally and instantaneously, raising to the q -power, expanding, and taking the conditional average yields

$$\langle \Phi_r^q | \epsilon_r \rangle = \sum_{n=0}^q \binom{q}{n} \epsilon_r^{q-n} \langle W_r^n | \epsilon_r \rangle. \quad (9)$$

Thus, for KRSJ to hold (i.e. for $\langle \Phi_r^q | \epsilon_r \rangle \propto \epsilon_r^q$) the conditional moments of W_r must follow the same behavior, i.e., $\langle W_r^n | \epsilon_r \rangle \propto \epsilon_r^n$. Both the KRSJ prediction for $\langle \Phi_r^q | \epsilon_r \rangle$ and $\langle W_r^n | \epsilon_r \rangle$ can be tested by measuring and plotting $\langle \Phi_r^q | \epsilon_r \rangle^{1/q}$ and $\langle W_r^n | \epsilon_r \rangle^{1/n}$ as function of ϵ_r and testing for linear behavior. Results are shown in Fig. 3 for $q = 2, 3$ and $n = 2, 3$. Clearly, the proportionality holds, with linear trends visible for every moment order over the range of dissipation values.

Given the success of the KRSJ and its implications in the context of the GKHE, it is worthwhile to examine other options. Note that the GKHE can also be conditionally averaged based on Φ_r instead of ϵ_r , and it reads

$$\left\langle \frac{\tilde{d}k_r}{dt} | \Phi_r \right\rangle = \Phi_r + \langle P_r | \Phi_r \rangle + \langle V_r | \Phi_r \rangle - \langle \epsilon_r | \Phi_r \rangle. \quad (10)$$

If one regards the energy cascade as proceeding “from large to small scales”, a causality argument might lead one to argue that the cascade rate Φ_r in the inertial range temporally precedes the dissipation ϵ_r , its ultimate fate

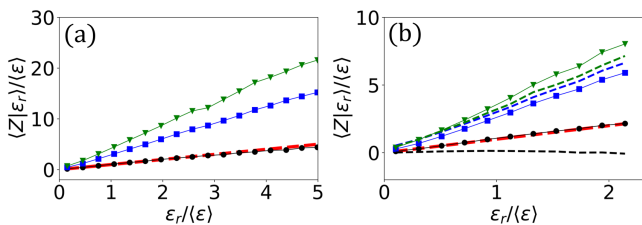


FIG. 3. Conditional averaged $Z = \Phi_r^n$ (symbols) for the isotropic8192 (a) and isotropic1024 (b) datasets, and $Z = W_r^n$ (dashed lines for the isotropic1024 dataset), for $r = 45\eta$, plotted as function of the conditioning variable ϵ_r . Results for $q = 1, 2, 3$ are shown in black, blue, and green respectively. All terms are normalized with $\langle \epsilon \rangle$ and display linear trends with ϵ_r , consistent with the KRSH.

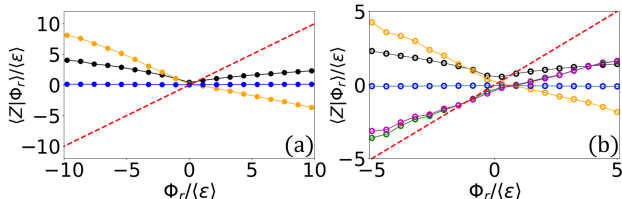


FIG. 4. Testing an “inverse KRSH”: plots of $Z = \epsilon_r$ (black circles and lines), $Z = \tilde{D}K_r/Dt$ (green circles and lines), $\langle P_r | \Phi_r \rangle$ (yellow circles and lines), $Z = V_r$ (blue circles and lines), and Φ_r (red dashed line) at $r = 0.0018\ell = 45\eta$ for the isotropic8192 (a) (without $Z = \tilde{D}K_r/Dt$) and at $r = 0.092\ell = 45\eta$ for the isotropic1024 data (b). Pink circles and lines are the sum on the RHS Eq. 10. All terms are normalized with $\langle \epsilon \rangle$.

due to viscosity. Therefore, one would be tempted to assume that *given* a value of Φ_r , the conditional average of ϵ_r given Φ_r will ultimately equal Φ_r (at least when it is positive). As argued in [24] such reasoning is also relevant to subgrid modeling, in which one knows velocity increments in the inertial range but the dissipation needs to be modeled. Hence, we wish to examine whether $\langle \epsilon_r | \Phi_r \rangle = \Phi_r$, which from Eq. 10 would also imply that $\langle W_r | \Phi_r \rangle \approx 0$ in the inertial range.

Figure 4 shows the measured terms in equation 10, using the isotropic8192 data in panel (a), and using isotropic1024 data including the unsteadiness (rate of change) term in panel (b) for $r = 45\eta$. Results for other r values (not shown) are very similar. We can see from the large differences between the circles with the red dashed line that an “inverse KRSH” does not hold. This result is consistent with earlier experimental results [24]. While their results showed good agreement with KRSH when evaluating the conditional average of the inertial range kinetic energy given the 1D surrogate of ϵ_r , an inverse KRSH (given the inertial range kinetic energy K_r , the conditionally averaged ϵ_r is supposed to scale as $K_r^{3/2}$) did not hold true. Here we are able to determine that the imbalance is due to the pressure $\langle P_r | \Phi_r \rangle$ and rate of change $\langle \tilde{d}K_r/dt | \Phi_r \rangle$ terms that do not vanish when conditioning based on Φ_r (recall that these terms were negligible when conditioning on ϵ_r).

The observed trends are physically plausible: $\langle \tilde{d}K_r/Dt | \Phi_r \rangle$ has the same sign as Φ_r , indicating small scales are gaining energy within the r -sphere when there is forward cascade to small scales, while during local inverse cascade events ($\Phi_r < 0$) the small scales lose kinetic energy. Finally regarding figure 4, we note that the good agreement between the unsteadiness term (green triangles) and total right hand side of Eq. 10 (pink triangles) shows that the budget of measured terms in Eq. 10 is complete. The conditional dissipation $\langle \epsilon_r | \Phi_r \rangle$ is non-negative, as expected, and it inflects at $\Phi_r = 0$ with different slopes for the positive and negative sides.

Having illustrated that conditioning based on ϵ_r is special (as foreseen by Kolmogorov 1962) and that not any dimensionally reasonable variable can be used successfully, we return to additional consequences of the original RKS. If any statistical property of velocity increments are only determined by the scale and ϵ_r (with a random prefactor V_Φ), then a further implication of RKS is that the conditional average of only positive and only negative values of Φ_r should also be proportional to ϵ_r (with their weighted sum being equal to ϵ_r). To investigate this prediction, we split the samples of Φ_r by its sign and perform conditional averaging based on ϵ_r . We first observe that there are about twice as many samples with $\Phi_r > 0$ than with $\Phi_r < 0$, specifically, if $P(\Phi_r > 0 | \epsilon_r)$ and $P(\Phi_r < 0 | \epsilon_r)$ are the conditional total probabilities associated with signs of Φ_r in any ϵ_r bin, we measure $P(\Phi_r > 0 | \epsilon_r) / P(\Phi_r < 0 | \epsilon_r) \approx 2.0$ (see blue line in Fig. 5, where at large ϵ_r there is evidence of saturation and the ratio decreases below 2). In the inertial range, the ratio is approximately 2.0 (consistent with results from Ref. [25], who defined energy cascade rate by detailed evaluations of intersection of eddies and lifetimes). From normalization we conclude that since $P(\Phi_r \geq 0) + P(\Phi_r < 0) = 1$, $P(\Phi_r > 0 | \epsilon_r) \approx 2/3$ and $P(\Phi_r < 0 | \epsilon_r) \approx 1/3$. And since $\langle \Phi_r | \epsilon_r \rangle = \langle \Phi_r | \epsilon_r, \Phi_r > 0 \rangle P(\Phi_r > 0 | \epsilon_r) + \langle \Phi_r | \epsilon_r, \Phi_r < 0 \rangle P(\Phi_r < 0 | \epsilon_r)$ and the data already showed $\langle \Phi_r | \epsilon_r \rangle \approx \epsilon_r$, the KRSH further implies that $\langle \Phi_r | \epsilon_r, \Phi_r < 0 \rangle \approx 3\epsilon_r - 2\langle \Phi_r | \epsilon_r, \Phi_r > 0 \rangle$. These predictions from RKS are tested in Fig. 5, showing that $\langle \Phi_r | \epsilon_r, \Phi_r < 0 \rangle \approx 2\epsilon_r$ and $\langle \Phi_r | \epsilon_r, \Phi_r < 0 \rangle \approx -1\epsilon_r$. Clearly KRSH holds even for the positive and negative regions separately. For completeness, we also show the conditional average of the traditional third-order longitudinal structure function, which under the assumption of isotropy is given by the 4/5-law, according to $\langle \Phi_r^{(L)} | \epsilon_r \rangle = -(5/4r) \langle [(\delta u_j \hat{n}_j)^3]_{S_r} | \epsilon_r \rangle$. Note that isotropy holds for the conditional average but not for individual realizations, and so while $\Phi_r < 0$ can be unambiguously associated with a local negative flux of energy across scales (from Eq. 3), $\Phi_r^{(L)} < 0$ locally does not arise directly in the equation for local kinetic energy and thus lacks the clear physical interpretation of Φ_r .

In summary, we reformulated the KRSH involving the spherically averaged dissipation ϵ_r in the context of an equation derived exactly from the Navier-Stokes equations in which ϵ_r appears explicitly. Data from two

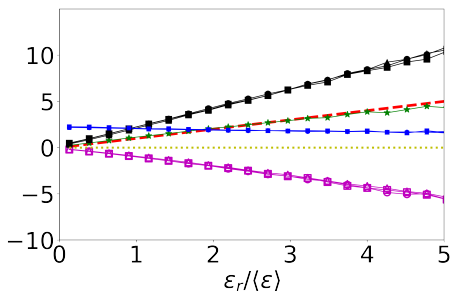


FIG. 5. Conditionally averaged positive (forward cascade, full symbols) and negative (inverse cascade, empty symbols) Φ_r for the isotropic8192 dataset, and for three scales r (symbols are the same as in Fig. 2). The blue symbols and line are the ratio of positive and negative realizations of cascade (≈ 2). The green stars show the standard 4/5-law quantity based on longitudinal structure function $\langle \Phi_r^{(L)} | \epsilon_r \rangle = -(5/4r) \langle [(\delta u_j \hat{n}_j)^3]_{S_r} | \epsilon_r \rangle$ showing good agreement with ϵ_r .

DNS forced isotropic turbulence, at intermediate and relatively high Reynolds numbers, were analyzed by explicitly evaluating local spherical volume and surface integrations at scales in the inertial range. The analysis provides strong support for the validity of KRSH not only for longitudinal velocity increments but also for moments of other terms appearing in the dynamical equation, i.e., the combined time rate of change and pressure work af-

fecting local kinetic energy in the inertial range of turbulence. When proposing an “inverse KRSH”, i.e. assuming we know the relevant cascade rate in the inertial range and wish to predict the locally averaged viscous dissipation (as one would wish to do e.g. in coarse-grained turbulence simulations at scale r in which dissipative scales are not resolved), predictions were clearly violated when confronted with data. Conversely, the data support a strong version of the KRSH when positive and negative cascade rates are considered separately, each of which scale proportional to ϵ_r . A KRSH connected directly to a dynamical equation may ultimately help advancing towards the goal of connecting, theoretically, the Navier-Stokes equations to the phenomenon of intermittency in the energy cascade. Also, it will be interesting to examine present results in light of the theorems presented in Refs. [19, 20]. If the latter are interpreted as implying that in the limit of infinite Reynolds number $\Phi_r \approx \epsilon_r$ locally without any conditional averaging (i.e. that $W_r/\epsilon_r \rightarrow 0$), then $\Phi_r < 0$ would become increasingly rare at large Reynolds number. Whether such a limit can be observed at finite Reynolds numbers remains an open question.

Acknowledgements: This work is supported by NSF (CSSI-2103874) and the contributions from the JHTDB team are gratefully acknowledged.

-
- [1] L. F. Richardson, *Weather prediction by numerical process* (Cambridge university press, 1922).
- [2] A. N. Kolmogorov, The local structure of turbulence in incompressible viscous fluid for very large Reynolds numbers, *Cr Acad. Sci. URSS* **30**, 301 (1941).
- [3] U. Frisch, *Turbulence: the legacy of AN Kolmogorov* (Cambridge university press, 1995).
- [4] A. N. Kolmogorov, A refinement of previous hypotheses concerning the local structure of turbulence in a viscous incompressible fluid at high Reynolds number, *Journal of Fluid Mechanics* **13**, 82 (1962).
- [5] C. Meneveau and K. R. Sreenivasan, The multifractal nature of turbulent energy dissipation, *Journal of Fluid Mechanics* **224**, 429 (1991).
- [6] G. Stolovitzky, P. Kailasnath, and K. R. Sreenivasan, Kolmogorov’s refined similarity hypotheses, *Physical review letters* **69**, 1178 (1992).
- [7] A. A. Praskovskiy, Experimental verification of the Kolmogorov refined similarity hypothesis, *Physics of Fluids A: Fluid Dynamics* **4**, 2589 (1992).
- [8] L.-P. Wang, S. Chen, J. G. Brasseur, and J. C. Wyngaard, Examination of hypotheses in the Kolmogorov refined turbulence theory through high-resolution simulations. part 1. velocity field, *Journal of Fluid Mechanics* **309**, 113 (1996).
- [9] K. P. Iyer, K. R. Sreenivasan, and P. K. Yeung, Refined similarity hypothesis using three-dimensional local averages, *Physical Review E* **92**, 063024 (2015).
- [10] J. M. Lawson, E. Bodenschatz, A. N. Knutsen, J. R. Dawson, and N. A. Worth, Direct assessment of Kolmogorov’s first refined similarity hypothesis, *Physical Review Fluids* **4**, 022601 (2019).
- [11] R. J. Hill, Equations relating structure functions of all orders, *Journal of Fluid Mechanics* **434**, 379 (2001).
- [12] R. J. Hill, Exact second-order structure-function relationships, *Journal of Fluid Mechanics* **468**, 317 (2002).
- [13] A. S. Monin and A. M. Yaglom, *Statistical Fluid Mechanics: Mechanics of Turbulence* (MIT Press, 1975).
- [14] L. Danaila, F. Anselmet, T. Zhou, and R. A. Antonia, Turbulent energy scale budget equations in a fully developed channel flow, *Journal of Fluid Mechanics* **430**, 87–109 (2001).
- [15] L. Danaila, F. Anselmet, and T. Zhou, Turbulent energy scale-budget equations for nearly homogeneous sheared turbulence, *Flow, Turbulence and Combustion*, 287–310 (2004).
- [16] L. Danaila, J. Krawczynski, F. Thiesset, and B. Renou, Yaglom-like equation in axisymmetric anisotropic turbulence, *Physica D: Nonlinear Phenomena* **241**, 216 (2012).
- [17] R. A. Antonia, M. Ould-Rouis, F. Anselmet, and Y. Zhu, Analogy between predictions of Kolmogorov and Yaglom, *Journal of Fluid Mechanics* **332**, 395–409 (1997).
- [18] R. A. Antonia, T. Zhou, L. Danaila, and F. Anselmet, Streamwise inhomogeneity of decaying grid turbulence, *Physics of Fluids* **12**, 3086 (2000).
- [19] J. Duchon and R. Robert, Inertial energy dissipation for weak solutions of incompressible euler and Navier-Stokes equations, *Nonlinearity* **13**, 249 (2000).
- [20] G. L. Eyink, Local 4/5-law and energy dissipation anomaly in turbulence, *Nonlinearity* **16**, 137 (2002).

- [21] B. Dubrulle, Beyond Kolmogorov cascades, *Journal of Fluid Mechanics* **867**, P1 (2019).
- [22] Y. Li, E. Perlman, M. Wan, Y. Yang, C. Meneveau, R. Burns, S. Chen, A. Szalay, and G. Eyink, A public turbulence database cluster and applications to study lagrangian evolution of velocity increments in turbulence, *Journal of Turbulence* , N31 (2008).
- [23] P. K. Yeung, X. Zhai, and K. R. Sreenivasan, Extreme events in computational turbulence, *Proceedings of the National Academy of Sciences* **112**, 12633 (2015).
- [24] C. Meneveau and J. O’Neil, Scaling laws of the dissipation rate of turbulent subgrid-scale kinetic energy, *Physical Review E* **49**, 2866 (1994).
- [25] J. I. Cardesa, A. Vela-Martín, and J. Jiménez, The turbulent cascade in five dimensions, *Science* **357**, 782 (2017).